RESEARCH PAPERS

Structural Model of the Orthorhombic Non-Fibonacci Approximant in the $Al_{12}Fe_2Cr$ Alloy

H. X. Sui,[a] X. Z. Liao,[a] K. H. Kuo,[a]* Xiaodong Zou[b] and Sven Hovmöller[b]

[a]*Beijing Laboratory of Electron Microscopy, Chinese Academy of Sciences, PO Box 2724, 100080 Beijing, People's Republic of China, and* [b]*Structural Chemistry, Stockholm University, S-106 91 Stockholm, Sweden. E-mail:khkuo@image.blem.ac.cn*

Abstract

$Al_{5.103}(Fe,Cr)$, orthorhombic, *Imm2*, $a = 12.34$, $b = 12.41$, $c = 30.71$ Å, $V = 4701$ Å³, atoms/cell = 305 (average), $D_x \simeq 3.4$ g cm⁻³. A structural model of the non-Fibonacci approximant O-AlFeCr with composition $Al_{5.103}(Fe,Cr)$ found in an $Al_{12}Fe_2Cr$ alloy has been derived from its high-resolution electron microscopy images and the structure of the hexagonal μ-Al_4Mn [Shoemaker, Keszler & Shoemaker (1989). *Acta Cryst.* B45, 13–20], being isostructural to μ-Al_4Cr. Among the 14 unique positions of transition metal (TM) atoms, 13 are icosahedrally coordinated: five of these icosahedra interpenetrate into each other, forming icosahedral chains along [010], and the remaining eight icosahedra with their twofold axis parallel to this axis. This structural model describes a (010) layer structure with a sequence $P^mFP(P^mFP)_I$, where a flat layer F (a mirror plane) is sandwiched between two puckered P and P^m layers, and $(P^mFP)_I$ is related to P^mFP through a body-centred translation. The interatomic distances are 2.51–2.74 Å for TM—TM, 2.38–2.99 for TM—Al and 2.41–3.18 Å for Al—Al. Simulated images and electron diffraction patterns calculated based on this structural model are comparable with the experimentally observed results.

1. Introduction

Most of the quasicrystal-related crystalline phases, or approximants, belong to the Fibonacci type (Elser & Henley, 1985; Ishii, 1989). In the case of Fibonacci approximants of the two-dimensional decagonal quasicrystals (DQC) the orthogonal lattice parameters a and c in the quasiperiodic plane perpendicular to the periodic tenfold **b** axis can be calculated from

$$a = 5^{1/2}a_R\tau^{n+1}/(1 + \tau^2)^{1/2} \qquad (1)$$

$$c = 5^{1/2}a_R\tau^{n'} \qquad (2)$$

by substituting a ratio of Fibonacci numbers for $\tau = (1 + 5^{1/2})/2 = 2\cos 36°$. Here $a_R = 4.0$–4.1 Å is the quasilattice constant or the edge length of the 36°

and 72° rhombi (Zhang & Kuo, 1990; Hu & Ryder, 1994), and n and n' are integers including zero.

Recently, we have reported a new type of decagonal approximant, the orthorhombic O-AlFeCr in the $Al_{12}Fe_2Cr$ alloy with lattice parameters $a = 12.3$, $b = 12.4$, $c = 30.7$ Å (Sui, Liao & Kuo, 1995), where c does not agree with any value calculated using (2). By analysing its electron diffraction patterns (EDP's) and high-resolution electron microscopy (HREM) images this compound is considered possibly to be a non-Fibonacci decagonal approximant. A phase with similar orthorhombic lattice parameters has also been found in $Al_{60}Mn_{11}Ni_4$ (Singh & Ranganathan, 1994), Al–Cu–Co–W (Liao, 1994) and Al–Cr–Ni (Rosell-Laclau, Durand-Charre & Audier, 1996) alloys, although no structural model has been given.

In the Al-rich Al–TM alloys there are a large number of complex crystal structures. By single crystal X-ray diffraction analysis some of these structures have been determined, such as $Al_{60}Mn_{11}Ni_4$ (Robinson, 1954), $Al_{13}Fe_4$ (Black, 1955a,b), φ-$Al_{10}Mn_3$ (Taylor, 1959), T_3-(AlMnZn) (Damjanovic, 1961), $Al_{13}Co_4$ (Hudd & Taylor, 1962), α-AlMnSi (Cooper & Robinson, 1966), α-AlFeSi (Cooper, 1967), μ-Al_4Mn (Shoemaker, Keszler & Shoemaker, 1989), Z-$Al_{59}Cu_5Li_{26}Mg_{10}$ (Le Bail, Leblanc & Audier, 1991), $Al_{61.3}Cu_{7.4}$-$Fe_{11.1}Cr_{17.2}Si_3$ (Kang, Malaman, Venturini & Dubois, 1992), λ-Al_4Mn (Franzen & Kreiner, 1993), O-$Al_{13}Co_4$ (Grin, Burkhardt, Ellner & Peters, 1994), Al_3Mn or Y-Al_4Mn (Shi, Li, Ma & Kuo, 1994) and Al_3Pd (Matsuo & Hiraga, 1994) *etc.* These crystalline phases are structurally related to quasicrystals and one of the common features is the icosahedral coordination of the majority of TM atoms. Sometimes the structure of a crystal with a smaller unit cell can even be a structural subunit of a larger unit cell, such as the structure of the hexagonal φ-$Al_{10}Mn_3$ with $a = 7.543$, $c = 7.898$ Å (Taylor, 1959), which can be found in hexagonal μ-Al_4Mn with $a = 19.98$, $c = 24.673$ Å (Shoemaker, Keszler & Shoemaker, 1989). Structural models of several highly complicated phases have been deduced from previously solved structures. For example, a

structural model for the orthorhombic Al_3Co was proposed (Li, Ma & Kuo, 1993, 1994) by introducing successively (100) faults into the unit cell of the monoclinic $Al_{13}Co_4$ structure determined by Hudd & Taylor (1962). This structural model was close to that obtained by X-ray single crystal diffraction analysis (Grin, Burkhardt, Ellner & Peters, 1994). A structural model of the orthorhombic Al_4Mn has also been derived (Li, Shi & Kuo, 1992) by rearranging the hexagonal subunits in the $Al_{60}Mn_{11}Ni_4$ unit cell determined by Robinson (1954). Hiraga, Kaneko, Matsuo & Hashimoto (1993) independently obtained a similar structure using HREM. A possible structural model has also been constructed for the C_{31}-$Al_{60}Mn_{11}Ni_4$ phase (Sui, Sun & Kuo, 1997) found by Van Tendeloo, Van Landuyt, Amelinckx & Ranganathan (1988). Sun, Yubuta & Hiraga (1995) found a different arrangement of atoms in a unit cell of the Al-Pd-Cr phase with about the same orthorhombic lattice parameters as C_{31}-$Al_{60}Mn_{11}Ni_4$. From the above evidence it perhaps can be concluded that the structure of an unknown approximant might be derived from a closely related known structure.

The hexagonal μ-Al_4Mn phase is an important approximant of quasicrystals (Audier & Guyot, 1986; Bendersky, 1987; Shoemaker, Keszler & Shoemaker, 1989; Shoemaker, 1993, 1994; Shoemaker & LeLann, 1993). The hexagonal μ-Al_4Cr (Kuo, 1990; Wen, Chen & Kuo, 1990, 1992; Bendersky, Roth, Ramon & Shechtman, 1991; Audier, Durand-Charre, Rosell-Laclau & Klein, 1995) is isostructural to it. In our attempt to solve the structure of the O-AlFeCr phase we looked at the chemically and structurally closely related compounds μ-Al_4Cr and μ-Al_4Mn. By analysing the high-resolution images of the orthorhombic O-AlFeCr its local structural arrangement was found to be similar to that of the projected structure of the hexagonal μ-Al_4Mn phase along its pseudo-tenfold axis (Shoemaker, 1993). A possible structural model of O-AlFeCr has thus been derived from the structure of the hexagonal μ-Al_4Mn and the result is presented below.

2. Experimental

The $Al_{12}Fe_2Cr$ alloy was prepared by melting a mixture of high purity Al (99.9999 wt%), Fe (99.5 wt%) and Cr (99.9 wt%) in an arc furnace. Thin samples for electron microscopy were prepared by slicing, grinding and ion milling. HREM images were taken with a JEOL 2010 electron microscope working at 200 kV with a point resolution of 1.94 Å. Selected-area electron diffraction patterns (EDP's) were taken with a Philips CM12 transmission electron microscope working at 120 kV. The HREM images were digitized using a scanmaker (MICROTEX MRS600-G). Areas of 512×512 pixels corresponding to 9.6 nm × 9.6 nm

at the thin edge of the crystal were selected for HREM images and these images were processed using the *CRISP* program (Hovmöller, 1992). Simulated HREM images were calculated (aperture 0.53 Å^{-1}, spherical aberration 0.5 mm, defocus spread 75 Å, specimen thickness ~ 10 nm) using the program kindly provided by Professor F. H. Li of the Institute of Physics, Chinese Academy of Sciences, based on the multi-slice method of Cowley & Moodie (1957). EDP's were
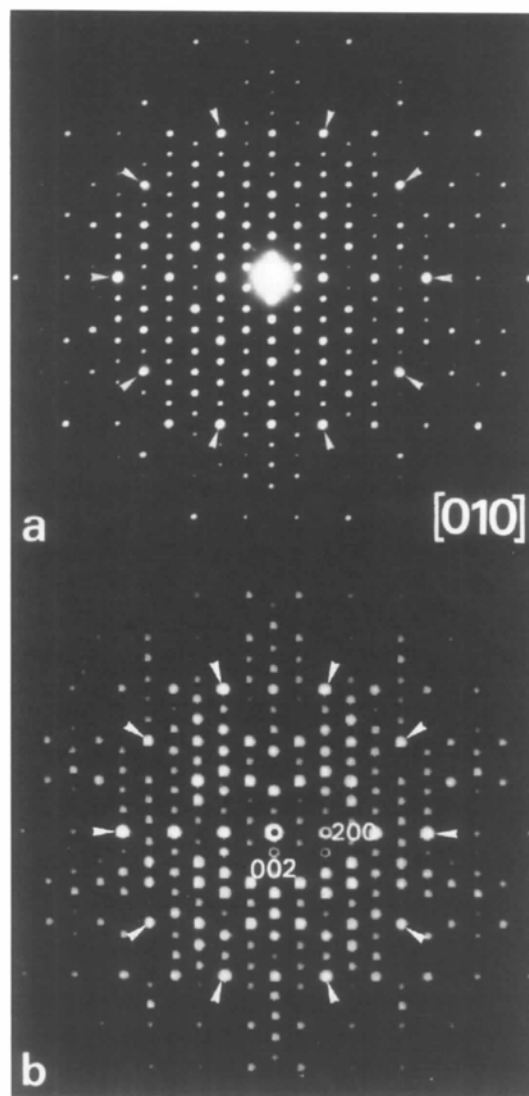

Fig. 1. (a) Experimental [010] EDP of the body-centred orthorhombic approximant O-AlFeCr, displaying a pseudo-decagon of strong diffraction spots (marked by arrows); (b) simulated [010] EDP based on the structure model (thickness 10 nm, 120 kV). The intensity distribution agrees in the main with that of the experimental displayed in Fig. 1(a), especially at higher resolution where the dynamical effects are less pronounced. Solid circles mark the diffraction spots corresponding to a centred rectangular reciprocal cell.

simulated using the *Macempas* program by Roa Kilaas.

3. Deducing a structural model

The [010] EDP of O-AlFeCr shows a pseudo-tenfold symmetry, Fig. 1(*a*). The characteristics of its [010] HREM image is a rhombic network of image points showing a strong bull's-eye contrast surrounded by ten small image points (see the sets of ten bright dots surrounding those strong image points marked with
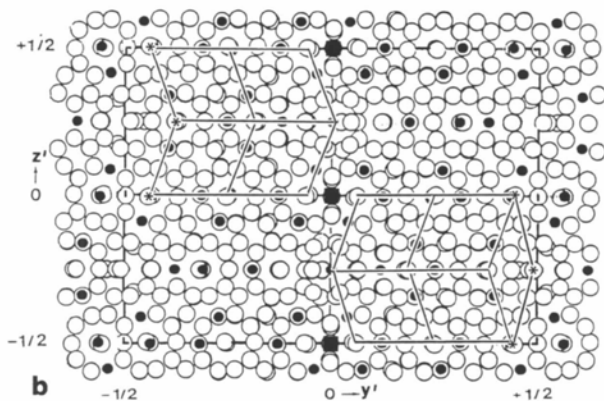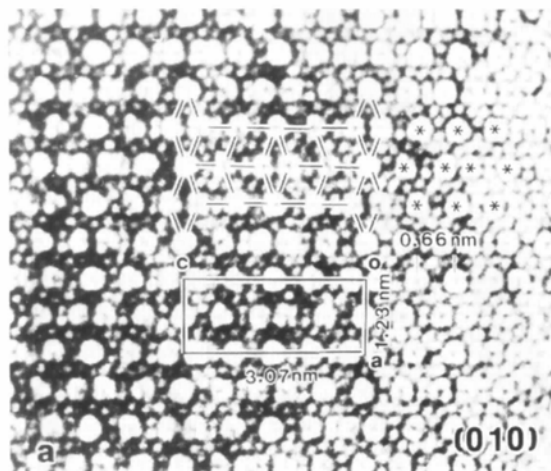

asterisks in Fig. 2*a*). A projected unit cell and the tiling of fat (72°) and thin (36°) rhombi in a unit cell are outlined. The centring comes from the projection of a body-centred unit cell. The edge length of these rhombi is 6.6 Å, being τ times larger than the quasilattice constant 4.0–4.1 nm in a DQC (Zhang & Kuo, 1990; Hu & Ryder, 1994).

The structure of the hexagonal μ-Al_4Mn (space group $P6_3/mmc$) was determined by Shoemaker, Keszler & Shoemaker (1989). Of the 110 Mn atoms 108 have icosahedral coordination with a coordination number (CN) 12 and two have CN 9. There are almost linear rows of interpenetrating icosahedra or pentagonal antiprisms in the ⟨100⟩ directions. In a discussion of its relationship to a DQC Shoemaker (1993) reset the hexagonal unit cell of μ-Al_4Mn as a C-centred orthorhombic one with space group $Cmcm$ and parameters $a' = a(\text{hex}) = 19.98$ (perpendicular to Fig. 2*b*), $b' = a(\text{hex}) \times 3^{1/2} = 34.61$ Å (horizontal in Fig. 2*b*), $c' = c(\text{hex}) = 24.673$ Å (vertical in Fig. 2*b*). The pseudo-tenfold [100] axis is then parallel to the a' axis, along which 16 atomic layers are stacked in a period of 19.98 nm. The five unique atomic layers are at $x' = 0$, $\sim 1/16$, $\sim 1/8$, $\sim 3/16$ and $\sim 1/4$, respectively. The remaining atomic layers can be obtained from these by symmetry operations across the mirror plane at $x' = 0$ and a glide plane at $x' = 1/4$.

We looked closer at the structure of μ-Al_4Mn and found it contains tilings similar to those which appeared in O-AlFeCr. The structural projection of μ-Al_4Mn along the pseudo-tenfold [100] axis (Fig. 2*b*), taken from Fig. 2 of Shoemaker (1993), shows rhombic subunits similar to those in the HREM image of the orthorhombic O-AlFeCr along its pseudo-tenfold **b** axis (Fig. 2*a*). The edge length of the rhombic tilings in μ-Al_4Mn is 6.6 Å, being the same as that of the O-AlFeCr phase. Furthermore, a local arrangement of the rhombic tilings (2×2 fat rhombi adjacent to one thin rhombus) can be found in both structures (see Fig. 2).

If we put the two outlined groups of 2×2 rhombi in Fig. 2(*b*) together by joining the atoms marked with asterisks, a rectangular cell (defined by the solid squares) consisting of eight fat and two thin rhombi is identical to that of O-AlFeCr (Fig. 2*a*). The length of the pseudo-tenfold axis of O-AlFeCr is 12.41 Å, whereas that of the μ-Al_4Mn phase is 19.98 Å. In μ-Al_4Mn there are five unique atomic layers: one flat mirror plane at $x' = 0$ and four puckered layers. In O-AlFeCr there should only be three unique layers: one flat mirror plane and two puckered layers. We could construct a plausible model of O-AlFeCr from the flat mirror plane and its two adjacent puckered layers in μ-Al_4Mn. Only a few minor adjustments were needed in order to avoid too short an interatomic distance.

The lattice parameter a in O-AlFeCr, 12.34 Å, is exactly half of $c' = 24.673$ Å in μ-Al_4Mn. The

Fig. 2. (*a*) The [010] HREM image of the O-AlFeCr phase, showing an arrangement of fat and thin rhombi whose edges are 0.66 nm. A (010) plane cell with $a = 12.3$, $c = 30.7$ Å is outlined. (*b*) The projection of the structure of μ-Al_4Mn along the pseudo-tenfold [100] axis [Fig. 2 in Shoemaker (1993)] shows rhombic subunits similar to those of the O-AlFeCr phase in (*a*). Solid circles are Mn atoms and open circles Al atoms. The outlined unit cell is $b' = 34.61$, $c' = 24.673$ Å. When the two parts consisting of 2×2 fat rhombi (one has also a thin rhombus) are joining together with the asterisks superimposed on each other, a rectangular plane cell consisting of eight fat and two thin rhombi results whose vertices are marked with squares.

Table 1. *Fractional atomic coordinates and occupancy factors for O-AlFeCr (TM = transition metal, Fe or Cr)*

	Sites	x	y	z	Occupancy
TM(1)	2(a)	0.0	0.0	0.1459	
TM(2)	4(c)	0.3242	0.0	0.2385	1.0
TM(3)	2(b)	1/2	0.0	0.0	1.0
TM(4)	2(b)	1/2	0.0	0.2907	1.0
TM(5)	2(a)	0.0	0.0	0.8541	1.0
TM(6)	4(c)	0.3242	0.0	0.7615	1.0
TM(7)	2(b)	1/2	0.0	0.7093	1.0
TM(8)	4(d)	0.0	0.1091	1/2	1.0
TM(9)	4(d)	0.0	0.1953	0.7160	1.0
TM(10)	4(d)	0.0	0.1953	0.2840	1.0
TM(11)	8(e)	0.1775	0.1910	0.0453	1.0
TM(12)	4(d)	1/2	0.1936	0.4280	1.0
TM(13)	4(d)	1/2	0.1990	0.8536	1.0
TM(14)	4(d)	1/2	0.1936	0.5720	1.0
Al(15)	2(a)	0.0	0.0	0.2923	1.0
Al(16)	2(a)	0.0	0.0	0.5790	1.0
Al(17)	4(c)	0.1151	0.0	0.4386	1.0
Al(18)	4(c)	0.1325	0.0	0.0	1.0
Al(19)	4(c)	0.1916	0.0	0.0898	1.0
Al(20)	4(c)	0.1813	0.0	0.1815	1.0
Al(21)	4(c)	0.3062	0.0	0.3278	1.0
Al(22)	4(c)	0.3869	0.0	0.1510	1.0
Al(23)	4(d)	1/2	0.0392	0.0766	0.4240
Al(24)	2(b)	1/2	0.0	0.4374	1.0
Al(25)	2(a)	0.0	0.0	0.7077	1.0
Al(26)	4(c)	0.1864	0.0	0.5291	1.0
Al(27)	4(c)	0.1836	0.0	0.9069	1.0
Al(28)	4(c)	0.1813	0.0	0.8185	1.0
Al(29)	4(c)	0.3062	0.0	0.6722	1.0
Al(30)	4(c)	0.3869	0.0	0.8490	1.0
Al(31)	4(c)	0.3500	0.0	0.9514	0.6720
Al(32)	2(b)	1/2	0.0	0.5626	1.0
Al(33)	4(d)	0.0	0.1018	0.0724	1.0
Al(34)	4(d)	0.0	0.1174	0.2090	1.0
Al(35)	8(e)	0.1151	0.1174	0.3537	1.0
Al(36)	8(e)	0.1790	0.1173	0.2632	1.0
Al(37)	8(e)	0.3467	0.1042	0.0267	0.6720
Al(38)	8(e)	0.3062	0.1157	0.4090	1.0
Al(39)	8(e)	0.3848	0.1196	1/2	1.0
Al(40)	4(d)	1/2	0.1031	0.2156	1.0
Al(41)	4(d)	1/2	0.1149	0.3543	1.0
Al(42)	4(d)	0.0	0.1018	0.9276	1.0
Al(43)	4(d)	0.0	0.1174	0.7910	1.0
Al(44)	8(e)	0.1151	0.1174	0.6463	1.0
Al(45)	8(e)	0.1790	0.1173	0.7368	1.0
Al(46)	8(e)	0.3062	0.1157	0.5910	1.0
Al(47)	4(d)	1/2	0.1031	0.7844	1.0
Al(48)	4(d)	1/2	0.1149	0.6457	1.0
Al(49)	4(d)	1/2	0.0969	0.9200	0.4240
Al(50)	4(d)	0.0	0.2037	0.0	1.0
Al(51)	4(d)	0.0	0.1872	0.4283	1.0
Al(52)	8(e)	0.1150	0.1910	0.1354	1.0
Al(53)	8(e)	0.1790	0.1911	0.4831	1.0
Al(54)	8(e)	0.3107	0.1846	0.1091	1.0
Al(55)	8(e)	0.3128	0.1890	0.1925	1.0
Al(56)	8(e)	0.3848	0.1850	0.2814	1.0
Al(57)	4(d)	1/2	0.1931	0.9941	0.4240
Al(58)	8(e)	0.1821	0.1850	0.9555	1.0
Al(59)	8(e)	0.1013	0.1760	0.5655	1.0
Al(60)	4(d)	1/2	0.1999	0.1344	1.0
Al(61)	8(e)	0.1150	0.1910	0.8646	1.0
Al(62)	8(e)	0.3188	0.1846	0.8965	1.0
Al(63)	8(e)	0.3128	0.1890	0.8075	1.0
Al(64)	8(e)	0.3848	0.1850	0.7186	1.0

structural model for O-AlFeCr has $c = 30.71\,\text{Å}$, which is shorter than the parameter $b' = 34.61\,\text{Å}$ of μ-Al_4Mn by a length of the shorter diagonal of the thin rhombus, Fig. 2(b). In reconstructing the unit cell of O-AlFeCr, a is reduced to half the original parameter c', therefore, the c glide mirror is lost.

On the other hand, a body centre has been found by electron diffraction analysis (Sui *et al.*, 1995). Therefore, the constructed structural model agrees with the space group *Imm2*. In the structure of μ-Al_4Mn the flat layer F at $x' = 0$ is a mirror m, whereas the next two (at $x' \sim 1/16$ and $\sim 1/8$) are puckered layers. These two puckered layers can be treated as one compound (P). Thus, the structural model of O-AlFeCr derived from the structure of μ-Al_4Mn can be described in terms of these layers stacked along the **b** axis in a $P^mFP(P^mFP)_I$ sequence, where the P^m layer is related to the P layer by a mirror reflection and $(P^mFP)_I$ is related to P^mFP by a body-centred translation.

4. Description of the structure model

4.1. Atomic sites

The atomic sites for O-AlFeCr (Table 1) were derived from those of the μ-Al_4Mn phase given by Shoemaker, Keszler & Shoemaker (1989). Only those atoms of μ-Al_4Mn in the subunit shown in Fig. 2(b) and located on the layers at $x' = 0$, $\sim 1/16$ and $\sim 1/8$ [see Figs. 1a–c in Shoemaker (1993)] were used. However, a few atoms in the neighbourhood of the junction of these two subunits were slightly adjusted or even removed in order to avoid too short a distance between the two atoms. There are 266 Al and 50 TM positions in a unit cell of O-AlFeCr (see Table 1). Among these, several Al positions are not fully occupied. In μ-Al_4Mn, with Al/Mn ratio 4.12, $Al(11)_\mu$ has an occupancy factor of 0.424. We have used the same occupancy factor for Al(23), Al(49) and Al(57) in our model of O-AlFeCr. For the same reason, Al(31) and Al(37) have an occupancy factor of 0.672, as does $Al(17)_\mu$. Therefore, the Al/TM ratio is not 266/50, but $255.15/50 = 5.103$, yielding a composition of $Al_{5.103}TM$.

4.2. Layer structure

The three unique layers perpendicular to the pseudo-tenfold [010] axis of the structural model of the O-AlFeCr phase at $y = 0$ (F layer), ~ 0.11 and ~ 0.19 are shown in Fig. 3. The flat layer at $y = 0$ (Fig. 3a) is a mirror, while the other two are puckered layers. In the flat layer, two Al(18), two Al(19), two Al(22), two Al(27) and two Al(30) form a decagon with TM(3) at its centre. Al(16), two Al(17) and two Al(26) form a pentagon surrounded by a large decagon consisting of Al(15), Al(21), Al(24), Al(25), Al(29) and Al(32). The puckered layer at $y \simeq 0.11$ is mainly composed of Al atoms (Fig. 3b) and the only TM atom is surrounded by an Al decagon. In the puckered layer at $y \simeq 0.19$ (Fig. 3c) there are also pentagons and decagons.

The O-AlFeCr phase can also be treated as a layered structure perpendicular to the [100] axis,
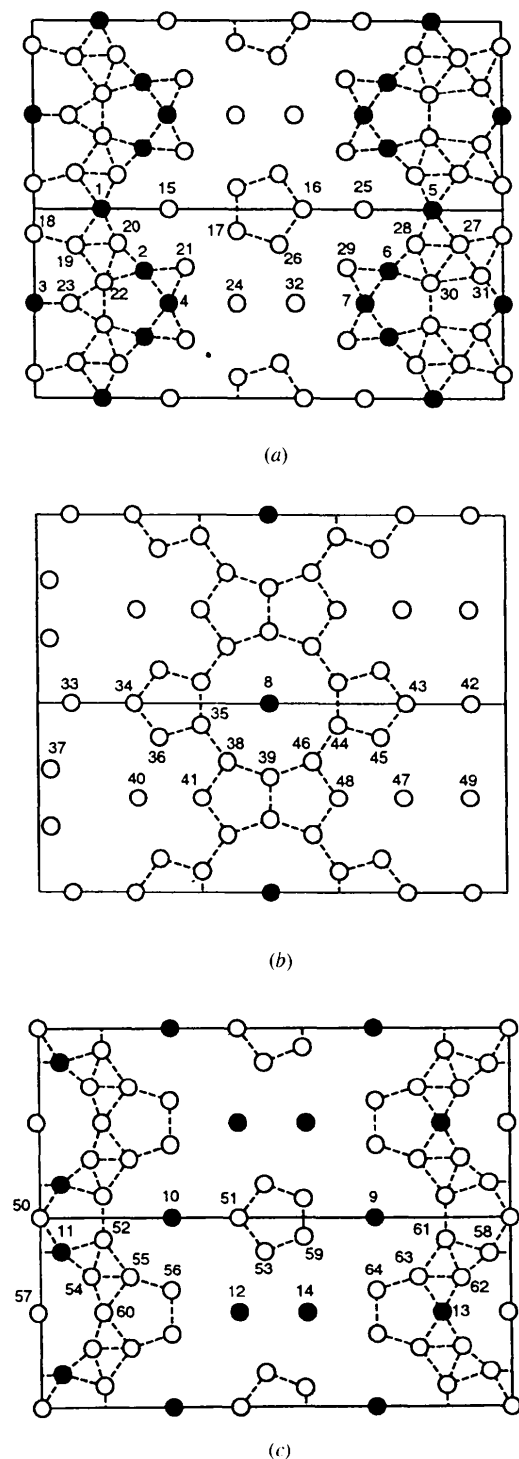
(a)

(b)

(c)

Fig. 3. The atomic layers of the structural model of O-AlFeCr perpendicular to the pseudo-tenfold [010] axis at (a) $y = 0$, (b) $y \simeq 0.11$ and (c) $y \simeq 0.19$, in which the filled circles are transition metal (TM) atoms (Fe or Cr) and the open circles Al atoms. The layer at $y = 0$ is a flat mirror, while the other two layers are puckered.

which corresponds to the c axis of the hexagonal μ-Al$_4$Mn. The (0001) layer structure has already been discussed in detail by Shoemaker, Keszler & Shoemaker (1989).

4.3. Icosahedral coordinations

Since the structure is derived from the μ-Al$_4$Mn phase (Shoemaker, Keszler & Shoemaker, 1989), most of the coordinations in the present model are similar to those in the μ-Al$_4$Mn phase. Among the 50 TM atoms, almost all have icosahedral coordination, except two TM(3) atoms which originate from the Mn(1)$_\mu$ position in the μ-Al$_4$Mn phase. For the TM(9), TM(10), TM(12), TM(14) and TM(8) atoms (altogether 20 in number) the pseudo-fivefold axis is parallel to the **b** direction of the O-AlFeCr phase. Fig. 4(a) shows an icosahedral chain along the pseudo-tenfold [010] axis, in which the right and left chains are of the same structure, but highlight different icosahedra to demonstrate the four interpenetrating icosahedra or four pentagonal antiprisms (PAP) with two pentagonal prisms (PP) at the two ends. In the [010] direction, four PAP's and 1 PP yield a **b** period of $\sim 2.95 + 2.35 \times 4 = 12.35$ Å, quite close to 1241 Å. Similar constructions also existed in the structure of μ-Al$_4$Mn (Shoemaker, Keszler & Shoemaker, 1989) and Al$_3$Mn (Hiraga, Kaneko, Matsuo & Hashimoto, 1993; Shi, Li, Ma & Kuo, 1994) with the 12.4 nm period along the pseudo-tenfold **b** direction.

For the other TM atoms the twofold axis, rather than the fivefold axis, is parallel to the [010] direction. Fig. 4(b) shows such an icosahedral coordination of TM(13) (with [010] perpendicular to the paper) linked with an icosahedral coordination of TM(10), whose fivefold axis is parallel to [010]. The 2 × Al(62) and 2 × Al(63) atoms are located at the same level as TM(13), which can also be seen in Fig. 3(c). Below this there is a rhombus consisting of Al(47) and Al(49) in Fig. 3(b) and 2 × Al(30) in Fig. 3(a). Above this there is a rhombus consisting of Al(15) in Fig. 3(a), 2 × Al(35) in Fig. 3(b) and Al(51) in Fig. 3(c). The Al coordinations are also similar to those in the μ-Al$_4$Mn phase. As seen in Fig. 4(a), Al(47) have icosahedral coordination, as do Al(33), Al(40) and Al(42). All these 16 Al atoms are located at centres of icosahedra aligned with their pseudo-fivefold axes parallel to the [010] direction of O-AlFeCr.

The atomic distances calculated from Table 1 are: TM—TM 2.51–2.74, TM—Al 2.38–2.99 and Al—Al 2.41–3.18 Å. The shortest distance for Al—TM 2.38 Å is between TM(3) and the partially occupied Al(31). In the structure of μ-Al$_4$Mn the shortest Al—Mn distance is 2.36 Å. Such short Al—TM distances have also been reported before in the structure of the T$_3$(AlMnZn) phase (Damjanovic, 1961) and the α(AlFeSi) phase (Cooper, 1967). In the structure of α(AlMnSi) (Cooper

& Robinson, 1966) the shortest Al—Mn distance is 2.27 Å. In the present model the shortest Al—Al distance of 2.41 Å is between two Al(49) positions which are partially occupied sites. Such a short Al—Al distance has also been reported by Cooper & Robinson (1966) in the α(AlMnSi) phase.

5. Verification of the model

The structural model of O-AlFeCr was verified by a qualitative comparison of experimental and calculated EDP's as well as experimental and simulated HREM
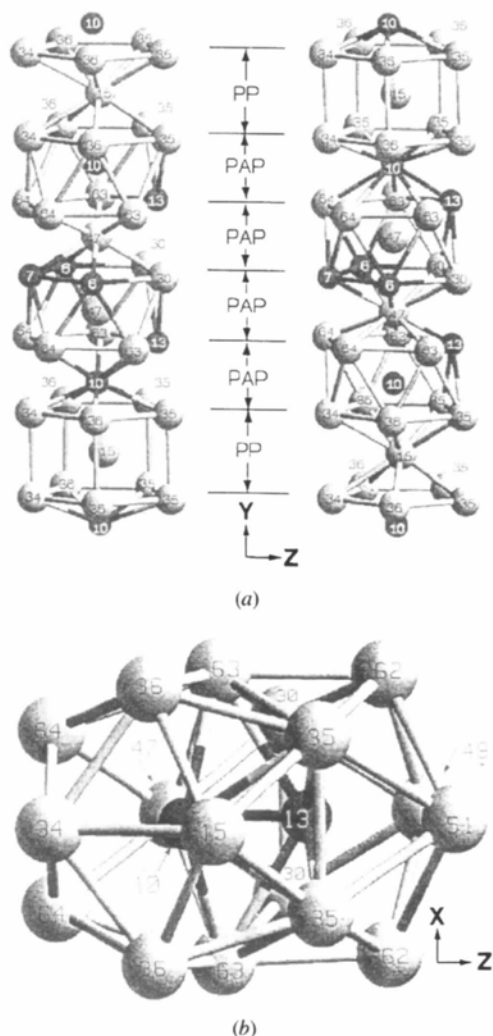

(a)

(b)

Fig. 4. Coordination polyhedra of O-AlFeCr: (a) A chain of four interpenetrated icosahedra in a b period: two of these icosahedra with TM(10) and Al(47) at the centres are highlighted on the left and the other two on the right, also with TM(10) and Al(47) at the centres. This can also be described as a chain of four pentagonal antiprisms (PAP) and one pentagonal prism (PP) over a period of 1.24 nm. (b) The icosahedral coordination of TM(13) with its twofold axis parallel to [010] links to a TM(10) icosahedron with its fivefold axis parallel to [010].

images. The calculated EDP's along [100], [010], [001] and some twofold axes agree in the main with the experimental results. The [010] EDP's are shown in Fig. 1.

HREM images along [010] and [100] were compared with simulated images calculated from the atomic parameters of the structural model listed in Table 1 (Figs. 5 and 6). It is well known that the image contrast of an HREM image changes dramatically with specimen thickness, specimen tilt and electron optical parameters, such as defocus and astigmatism *etc*. In general, a good match of a single pair of observed and simulated images may not be enough to establish the structural model used for this simulation. A good match in image contrast between a set of simulated images and the corresponding observed through-focus HREM images within a broad defocus range is more conclusive. Due to a rather high noise level and some crystal tilt, a direct comparison between the experimental and simulated HREM images was difficult. Both the noise and tilt effects can be compensated for by unit-cell averaging and the introduction of plane-group symmetry by means of the *CRISP* program (Hovmöller, 1992). Such processing improves the clarity of these images, but does not change their general appearance.

Three HREM images with different defocus values were taken along the pseudo-tenfold axis [010] (Figs. 5a, 5d and 5g). The plane-group symmetry *Cm* (a projection of the space-group symmetry *Imm*2) was imposed in Figs. 5(b), 5(e) and 5(h). The simulated images at these three defocus values −56, −64 and −80 nm, Figs. 5(c), 5(f) and 5(i), show similar structural characteristics as the processed images in Figs. 5(b), 5(e) and 5(h), respectively. Along [100] only one good image with a defocus value of −64 nm was obtained. Also in this case the simulated image agrees in the main with this observed image (Fig. 6). Among the 12 small bright points surrounding the strong blobs at the vertices and the centre of the rectangular cell, eight are strong, marked with solid circles in Figs. 6(b) and 6(c), and four at the 1, 5, 7 and 11 o'clock positions are weak.

6. Discussion and conclusions

In the present work a structural model of the orthorhombic O-AlFeCr has been presented. It is based on the structurally closely related hexagonal μ-Al$_4$Mn determined by Shoemaker, Keszler & Shoemaker (1989). In a b period of this model the icosahedral chain consists of four interpenetrating icosahedra displaying a pseudo-fivefold symmetry. The structural model contains 266 Al and 50 transitional metal positions in a unit cell with $a = 12.34$, $b = 12.41$, $c = 30.71$ Å. Simulated EDP's and HREM images

HREM Image   Processed Image   Simulated Image
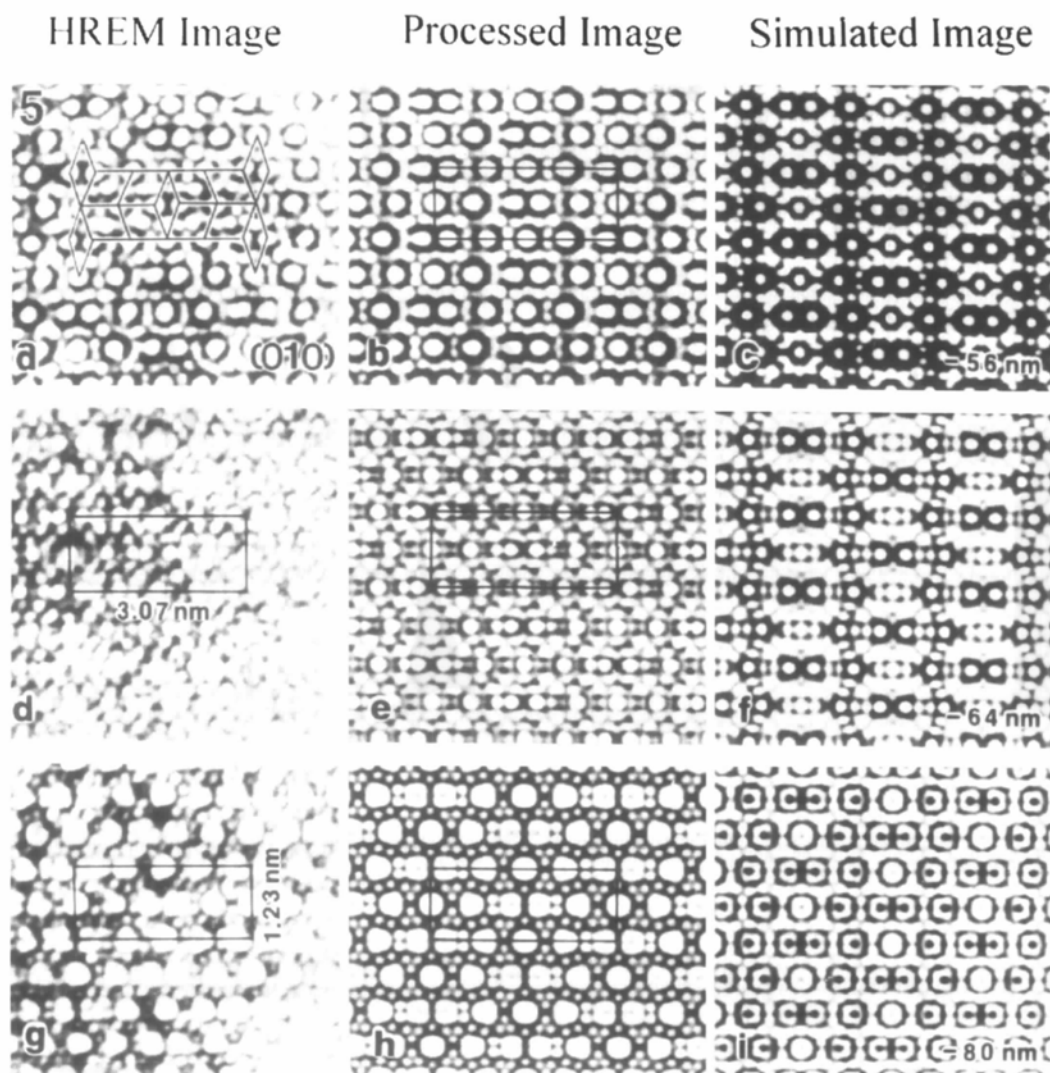

Fig. 5. Comparison of (a, d, g) experimental, (b, e, h) processed and (c, f, i) simulated HREM images along [010]. Three images of a through-focus series are shown. The image processing consists of unit-cell averaging and the introduction of the projected symmetry *Cm* by means of the *CRISP* program (Hovmöller, 1992). The crystal thickness used for simulation was 9.928 nm. The defocus values (-56, -64 and -80 nm) of the simulated images are marked at the bottom right corner of the images in the right column.
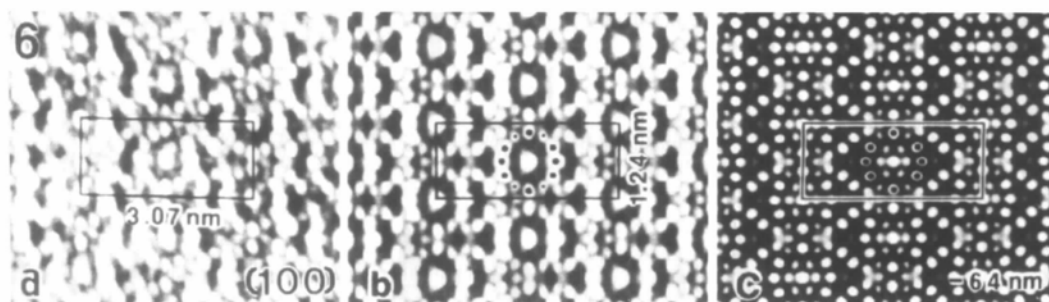
Fig. 6. Comparison of the (a) experimental, (b) processed and (c) simulated HREM images along [100]. The defocus value of the simulated image is -64 nm and the thickness for simulation 9.872 nm. Around the large blob in the centre and corners of the unit cell are 12 small bright points, both in the experimental and in the simulated image.

along [010] and [100] orientations are comparable with the experimental results.

We propose here that O-AlFeCr has *Imm*2 symmetry, being different from the *Immm* reported in a previous study (Sui, Liao & Kuo, 1995). As mentioned previously (Sui, Liao & Kuo, 1995), superstructure ordering frequently occurs in the O-AlFeCr phase. This ordering induces streaks occurring between the 00*l*, 01*l*, 02*l*, ... rows of spots in the c* direction in the [100] EDP and sometimes even causes diffuse scattering in the high-order diffraction spots. Such an ordering will create microdomains with (001) as a mirror plane. If an electron beam is incident on such a region, the convergent-beam electron diffraction pattern might show a mirror symmetry parallel to (001). Moreover, in our model most of the atoms are located at the position with almost *Immm* symmetry, except for a few atoms at $z \simeq 0$ or 0.5, which are the junction of the two subunits shown in Fig. 2(*b*). Some atomic clusters in the model can be rotated through 180° along the [010] orientation, causing only small changes in nearest-neighbour relations. For example, if the icosahedral cluster around TM(8) and the cluster around TM(3) are rotated through 180° along the [010] axis, there are almost no changes in the atomic nearest-neighbour environments. Similarly, the atoms TM(13) and Al(60), and TM(11) and Al(58) could also be interchanged. If both orientations were present, a mirror would be introduced perpendicular to c. Thus, the crystal might show an apparent space group of *Immm*. This possibility will be further investigated.

Among the 14 unique TM atoms in an O-AlFeCr unit cell 13 have icosahedral coordination; five of the 13 icosahedra are aligned with their pseudo-fivefold axis parallel to the pseudo-tenfold axis [010] and the other eight have their twofold axes parallel to [010]. For the four unique Al atoms with icosahedral coordination their pseudo-fivefold axes are all parallel to the pseudo-tenfold axis [010]. As suggested by Wen, Chen & Kuo (1992) for μ-Al_4Cr, the combination of the pseudo-fivefold and the twofold symmetries of these TM icosahedra will result in a pseudo-tenfold axis parallel to [010]. This also applies to the present case.

References

Audier, M., Durand-Charre, M., Rosell-Laclau, E. & Klein, H. (1995). *J. Alloys Compd.* **220**, 225–230.

Audier, M. & Guyot, P. (1986). *J. Phys. (Paris)*, **47**, Suppl. 3, C3-405–414.

Bendersky, L. (1987). *J. Microsc.* **146**, 303–312.

Bendersky, L., Roth, R. S., Ramon, J. T. & Shechtman, D. (1991). *Metall. Trans. A*, **22**, 5–10.

Black, P. J. (1955a). *Acta Cryst.* **8**, 43–48.

Black, P. J. (1955b). *Acta Cryst.* **8**, 175–182.

Cooper, M. (1967). *Acta Cryst.* **23**, 1106–1107.

Cooper, M. & Robinson, K. (1966). *Acta Cryst.* **20**, 614–617.

Cowley, J. M. & Moodie, A. F. (1957). *Acta Cryst.* **10**, 609–619.

Damjanovic, A. (1961). *Acta Cryst.* **14**, 982–987.

Elser, V. & Henley, C. L. (1985). *Phys. Rev. Lett.* **55**, 2883–2886.

Franzen, H. F. & Kreiner, G. (1993). *J. Alloys. Compd.* **202**, L21–L23.

Grin, J., Burkhardt, U., Ellner, M. & Peters, K. (1994). *J. Alloys Compd.* **206**, 243–247.

Hiraga, K., Kaneko, M. Matsuo, Y. & Hashimoto, S. (1993). *Philos. Mag. B*, **67**, 193–205.

Hovmöller, S. (1992). *Ultramicroscopy*, **41**, 121–135.

Hu, J. J. & Ryder, R. L. (1994). *Mater. Sci. Forum*, **150–151**, 235–246.

Hudd, R. C. & Taylor, W. H. (1962). *Acta Cryst.* **15**, 441–442.

Ishii, Y. (1989). *Phys. Rev. B*, **39**, 11862–11871.

Kang, S. S., Malaman, B., Venturini, G. & Dubois, J. M. (1992). *Acta Cryst.* **B48**, 770–776.

Kuo, K. H. (1990). *J. Less-Common Met.* **163**, 9–17.

Le Bail, A., Leblanc, M. & Audier, M. (1991). *Acta Cryst.* **B47**, 451–457.

Li, X. Z., Ma, X. L. & Kuo, K. H. (1993). *Acta Cryst.* **A49**, C342.

Li, X. Z., Ma, X. L. & Kuo, K. H. (1994). *Philos. Mag. Lett.* **70**, 221–229.

Li, X. Z., Shi, D. & Kuo, K. H. (1992). *Philos. Mag. B*, **66**, 331–340.

Liao, X. Z. (1994). Private communication.

Matsuo, Y. & Hiraga, K. (1994). *Philos. Mag. Lett.* **70**, 155–161.

Robinson, K. (1954). *Acta Cryst.* **7**, 494–497.

Rosell-Laclau, E., Durand-Charre, M. & Audier, M. (1996). *J. Alloys Compd.* **233**, 246–263.

Shi, N. C., Li, X. Z., Ma, Z. S. & Kuo, K. H. (1994). *Acta Cryst.* **B50**, 22–30.

Shoemaker, C. B. (1993). *Philos. Mag. B*, **67**, 869–881.

Shoemaker, C. B. (1994). *Mater. Sci. Forum*, **150–151**, 191–198.

Shoemaker, C. B., Keszler, D. A. & Shoemaker, D. P. (1989). *Acta Cryst.* **B45**, 13–20.

Shoemaker, C. B. & LeLann, A. (1993). *J. Non-Cryst. Solids*, **153/154**, 654–657.

Singh, A. & Ranganathan, S. (1994). *Mater. Sci. Eng.* **A181–A182**, 754–757.

Sui, H. X., Liao, X. Z. & Kuo, K. H. (1995). *Philos. Mag. Lett.* **71**, 139–145.

Sui, H. X., Sun, K. & Kuo, K. H. (1997). *Philos. Mag. A*, **75**, 379–393.

Sun, W., Yubuta, K. & Hiraga, K. (1995). *Philos. Mag. B*, **71**, 71–80.

Taylor, M. A. (1959). *Acta Cryst.* **12**, 393–396.

Van Tendeloo, G., Van Landuyt, J., Amelinckx, S. & Ranganathan, S. (1988). *J. Microsc.* **149**, 1–19.

Wen, K. Y., Chen, Y. L. & Kuo, K. H. (1990). *Quasicrystals*, edited by K. H. Kuo & T. Ninimiya, pp. 134–141. Singapore: World Scientific.

Wen, K. Y., Chen, Y. L. & Kuo, K. H. (1992). *Metall. Trans. A*, **23**, 2437–2444.

Zhang, H. & Kuo, K. H. (1990). *Phys. Rev. B*, **42**, 8907–8914.